

Electronic Supplementary Information

Intracellular coassembly boosts the anti-inflammation capacity of dexamethasone

Wei Tang,^a Jingbo Yang,^b Zhibin Zhao,^b Zhexiong Lian,^b and Gaolin Liang^{*,a}

^aCAS Key Laboratory of Soft Matter Chemistry, Department of Chemistry, University of Science and Technology of China, Hefei, Anhui 230026, China.

^bLiver Immunology Laboratory, Institute of Immunology and School of Life Sciences, University of Science and Technology of China, Hefei, Anhui 230027, China.

*Corresponding author: gliang@ustc.edu.cn (G. L.).

Table of Contents

1. General methods

2. Syntheses and Characterizations of 1p and 1

3. Supporting figures and tables

1. General methods

Dexamethasone phosphate (**Dp**) and dexamethasone (**Dex**) was purchased from Shanghai Yuanye Co. Ltd., reagent grade or better. All the other starting materials were obtained from Adamas or GL Biochem. Commercially available reagents were used without further purification, unless noted otherwise. Recombinant intestinal alkaline phosphatase (ALP) was obtained from BaoMan Inc. (Shanghai, China) (one unit is the enzyme activity that cleaves 1 μmol of the standard substrate per minute at 37 °C). The phosphatase inhibitor complex II was bought from Sangong Biotech Inc. (Shanghai, China) (every 10 μL ALP inhibitor complex II in culture medium containing 1×10^7 cells). HPLC analyses were performed on a Shimadzu UFLC system equipped with two LC-20AP pumps and an SPD-20A UV/vis detector using a Shimadzu PRC-ODS column, or on an Agilent 1200 HPLC system equipped with a G1322A pump and an in-line diode array UV detector using an Agilent Zorbax 300SB-C18 RP column, with CH_3CN (0.1% of TFA) and ultrapure water (0.1% of TFA) as the eluent. Electrospray ionization (ESI) mass spectra were obtained on a Finnigan LCQ Advantage ion trap mass spectrometer (ThermoFisher Corporation). ^1H NMR and ^{13}C NMR spectra were obtained on a Bruker AV 300. Rheology measurements were performed on a Haake RheoStress 6000 (Thermo Scientific), with cone-and-plate geometry (1 deg/20 mm) at the gap of 50 μm . UV-vis spectra were obtained on a PerkinElmer Lambda 25 UV-vis spectrometer. Cryo transmission electron microscopy (cryo-TEM) images were obtained on a Tecnai F20 transmission electron microscope from FEI company, operating at 120 kV. MTT results were recorded on an IEMS Analyzer (Lab-system, Type 1401). Ultrapure water (18.2 $\text{M}\Omega\cdot\text{cm}$) was used throughout the experiment.

General procedures for hydrogel preparation

Two mg **1p**, or 2 mg **1p** with 1.4 mg **Dp** were dissolved in 200 μL phosphate buffer (0.2 M, pH 7.4),

then 40 units of ALP was added and the mixtures were incubated at 37 °C for 8 h to form the supramolecular hydrogels.

Bone marrow-derived macrophage culture

BMDMs were derived from C57BL/6 mice as described.¹ Mice were purchased from the Experimental Animal Center, Chinese Academy of Science (Shanghai, China). All animal procedures were performed in accordance with the Guidelines for Care and Use of Laboratory Animals of University of Science and Technology of China (USTC, China) and approved by the Animal Ethics of USTC Animal Care and Use Committee. Briefly, tibia and femoral bone marrow cells were isolated and cultured in DMEM complemented with 10% FBS in the presence of culture supernatants of L929 mouse fibroblasts.

Co-incubation experiments

BMDMs were divided into 4 groups: **1p** with **Dp**, **Dp**, **1p**, and positive control (**PC**). All groups were added with 200 ng/mL lipopolysaccharide (LPS) to stimulate the inflammatory phenotype of BMDMs. Different compounds at concentration of 25 μM were added into different groups and incubated with BMDMs for 24 h then analyzed with a FACSVerse flow cytometer.

Flow cytometry

Cell suspensions were incubated with anti-mouse CD16/32 (Biolegend, San Diego, CA) to block the Fc receptor before cell surface staining. All flow antibodies, unless otherwise noted, were purchased from Biolegend. To identify phenotypes and functional indexes of BMDMs, cells were stained with FITC-MHC-II (M5/114.15.2), PerCP-Cy5.5-CD11c (N418), PE/Cy7-CD80 (16-10A1), APC-F4/80 (CD8A), APC-Cy7-CD86 (GL1), V500-CD11b (M1/70). Normal IgG isotype controls (Biolegend) were used as controls. Flow data were acquired on a flow cytometer FACSVerse (BD Bioscience).

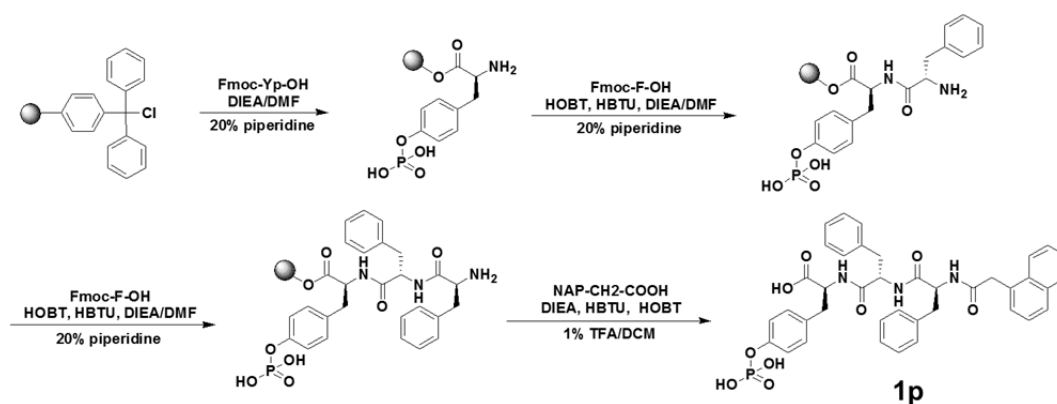
Data were analyzed with Flow Jo software (Tree Star, Inc., Ashland, OR).

MTT assay

The 3-(4, 5-dimethylthiazol-2-yl)-2, 5-diphenyltetrazolium bromide (MTT) assay on BMDMs was used to measure the cytotoxicity. Cells were seeded into 96-well cell-culture plate at 5×10^4 /well. The cells were incubated at 37 °C under 5% CO₂. The solutions of compounds diluted by DMEM (100 μL/well) at concentrations of 3.125, 6.25, 12.5, 25, 50, or 100 μM in 100 μL medium were added to the wells, respectively. The cells were incubated for 12, 24, or 48 h at 37 °C under 5% CO₂. A solution of 5 mg/mL MTT dissolved in phosphate buffered saline (PBS) (pH 7.4) (10 μL/well) was added to each well of the 96-well plate. A solution of DMSO (100 μL/well) was added to dissolve the formazan after an additional 10-minute shaking. The data were obtained using an ELISA reader (VARIOSKAN FLASH) to detect its absorption at 490 nm. Each of the experiments was performed at least three times.

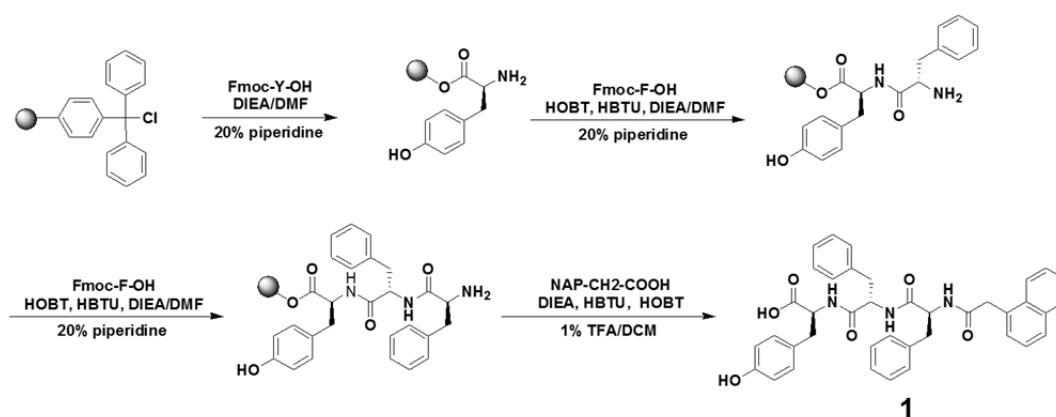
2. Syntheses and Characterizations of **1p** and **1**.

Scheme S1. The synthesis route for **1P**.



Synthesis of 1P: Compound 1-Nap-Phe-Phe-Tyr(H₂PO₃)-OH (**1P**) was synthesized with solid phase peptide synthesis (SPPS) and purified with HPLC. ¹H NMR (300 MHz, DMSO-*d*₆) δ 8.34 (dd, *J* = 12.4, 8.0 Hz, 2 H), 8.17 (d, *J* = 8.1 Hz, 1 H), 7.91 – 7.70 (m, 3 H), 7.40 (ddd, *J* = 29.7, 14.9, 7.4 Hz, 3 H), 7.28 – 7.13 (m, 10 H), 7.08 (d, *J* = 8.2 Hz, 2 H), 4.61 – 4.41 (m, 3 H), 3.79 (s, 2 H), 3.10 – 2.84 (m, 6 H), 2.75 (dt, *J* = 14.8, 6.7 Hz, 2 H) (Figure S1). ¹³C NMR (75 MHz, DMSO-*d*₆) δ 172.54, 171.05 (2C), 171.00, 150.28, 137.75, 137.50, 133.15, 132.66, 132.43, 129.18 (3C), 128.17 (5C), 127.96 (4C), 127.87, 127.58, 126.86, 126.20, 126.08, 125.83, 125.44 (2C), 119.79 (2C), 53.58 (3C), 37.48 (3C), 35.91 (Figure S2). ³¹P NMR of **1p** (*d*₆-DMSO, 162 MHz) δ (ppm): -6.13. (Figure S3). MS: calculated for C₃₉H₃₈N₃O₉P [(M+H)⁺]: 724.24, obsvd. ESI-MS: *m/z* 724.14 (Figure S4).

Scheme S2. The synthesis route for **1**.



Synthesis of 1: Compound 1-Nap-Phe-Phe-Tyr-OH (**1**) was synthesized after deprotection of the protecting group from 1-Nap-Phe-Phe-Tyr(tBu)-OH, which was synthesized with SPPS and purified by HPLC. ^1H NMR (300 MHz, $\text{DMSO-}d_6$) δ 8.35 – 8.08 (m, 3 H), 7.97 – 7.72 (m, 3 H), 7.39 (ddd, J = 29.7, 14.9, 7.4 Hz, 3 H), 7.18 (d, J = 11.2 Hz, 10 H), 7.03 (d, J = 8.1 Hz, 2 H), 6.66 (d, J = 8.1 Hz, 2 H), 4.54 (tdd, J = 12.8, 8.8, 4.0 Hz, 2 H), 4.39 (q, J = 7.3 Hz, 1 H), 3.81 (q, J = 15.2 Hz, 2 H), 2.87 (dd, J = 29.8, 5.1 Hz, 4 H), 2.71 (s, 2 H) (Figure S5). ^{13}C NMR (75 MHz, $\text{DMSO-}d_6$) δ 172.74, 170.98 (2C), 170.83, 155.93, 137.75, 137.49, 133.15, 132.43, 131.82, 130.02 (3C), 129.20 (5C), 129.17 (4C), 128.17, 127.94, 127.87, 127.57, 127.26, 126.85, 124.11 (2C), 114.98 (2C), 53.79, 53.63, 53.56, 37.51, 35.96 (2C), 35.73 (Figure S6). MS: calculated for $\text{C}_{39}\text{H}_{37}\text{N}_3\text{O}_6$ [(M+H) $^+$]: 644.28, obsvd. ESI-MS: m/z 644.06 (Figure S7).

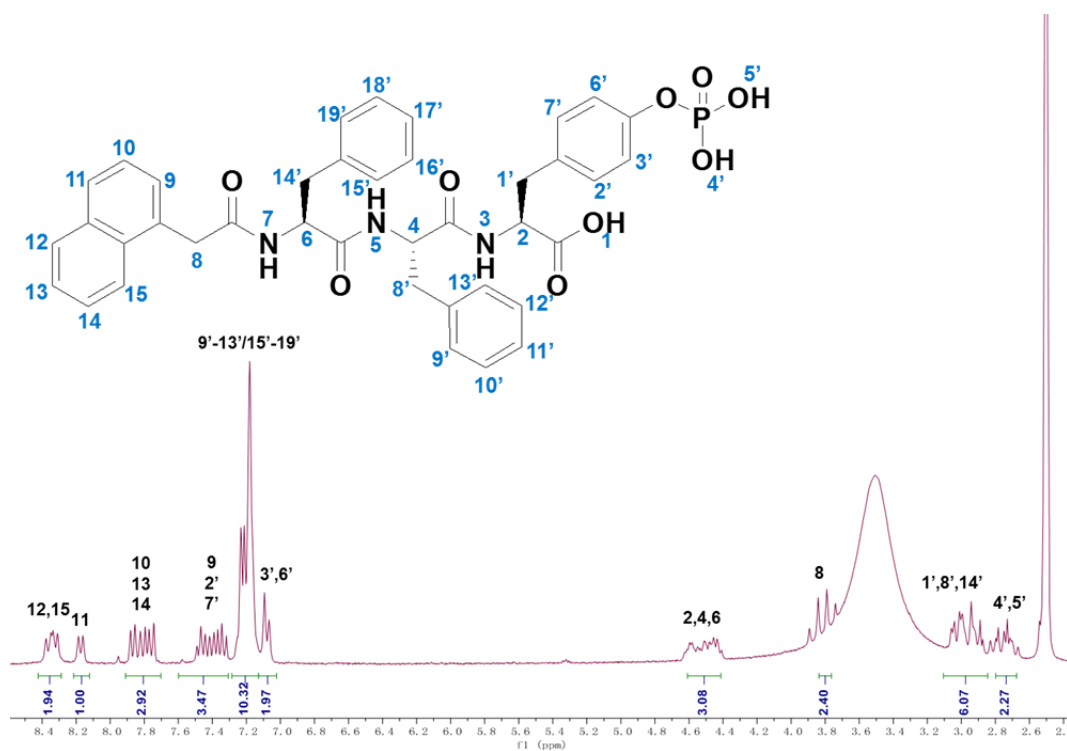


Figure S1. ^1H NMR spectrum of **1P**.

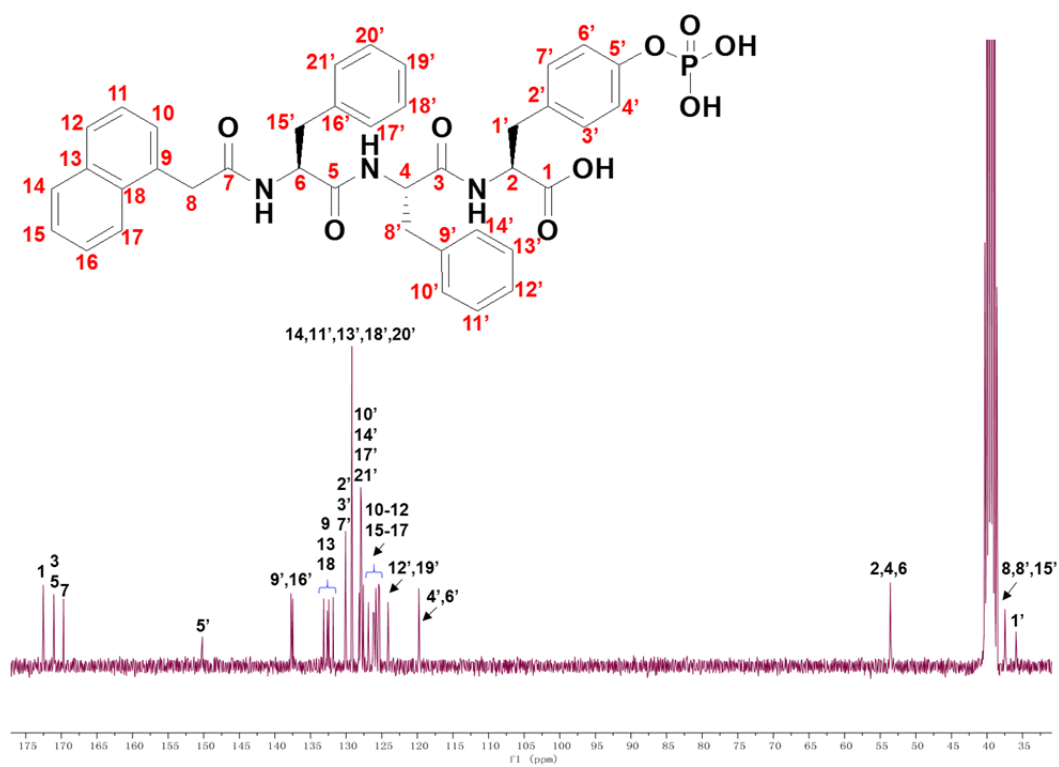


Figure S2. ^{13}C NMR spectrum of **1P**.

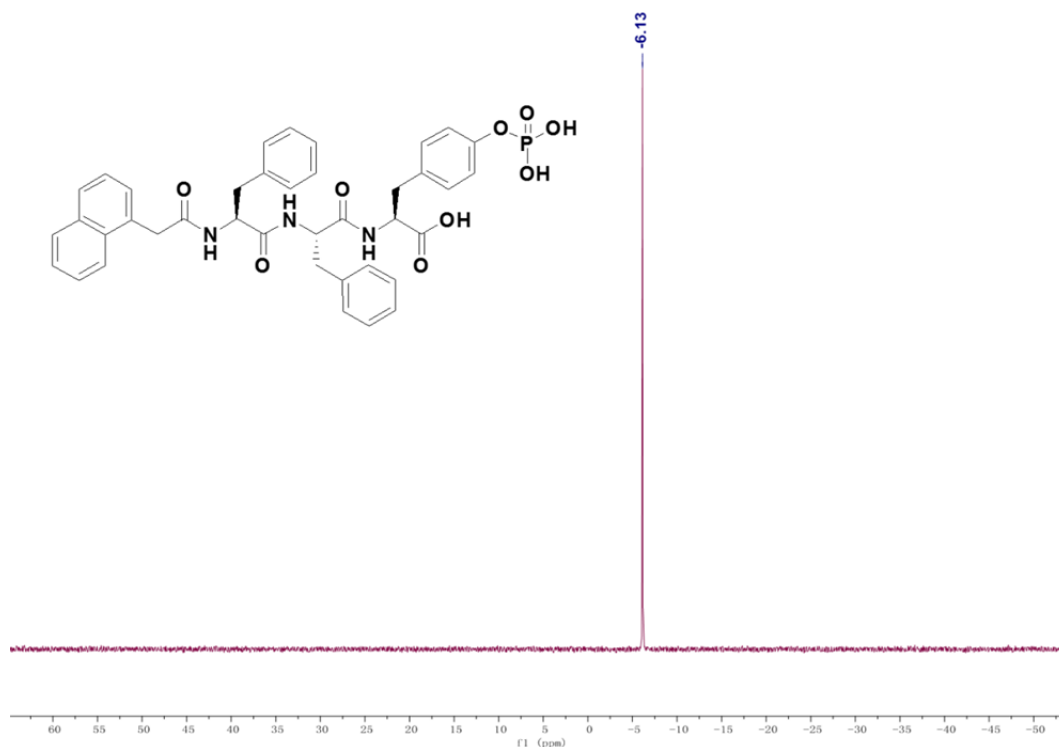


Figure S3. ^{31}P NMR spectrum of **1p**.

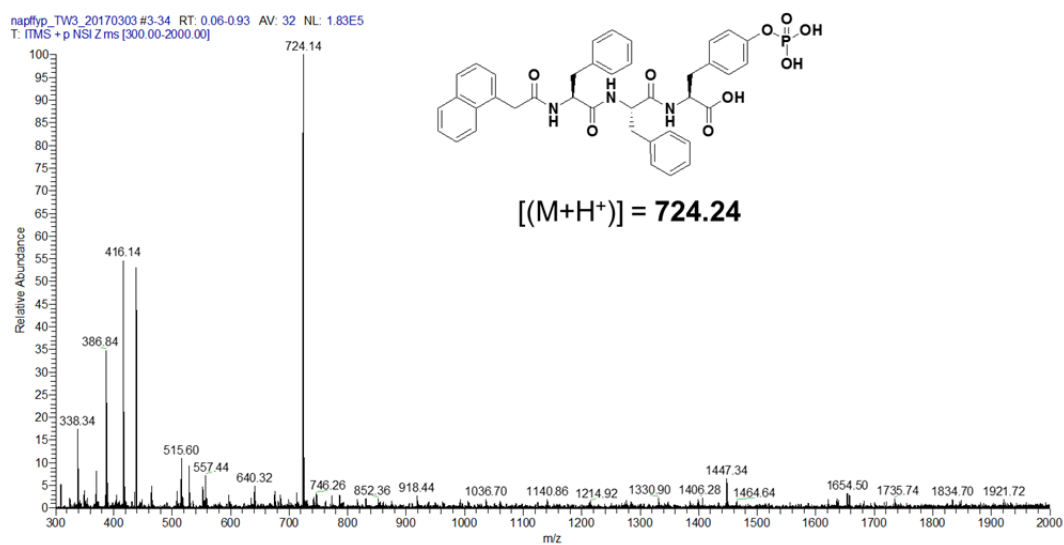


Figure S4. ESI-MS spectrum of **1p**.

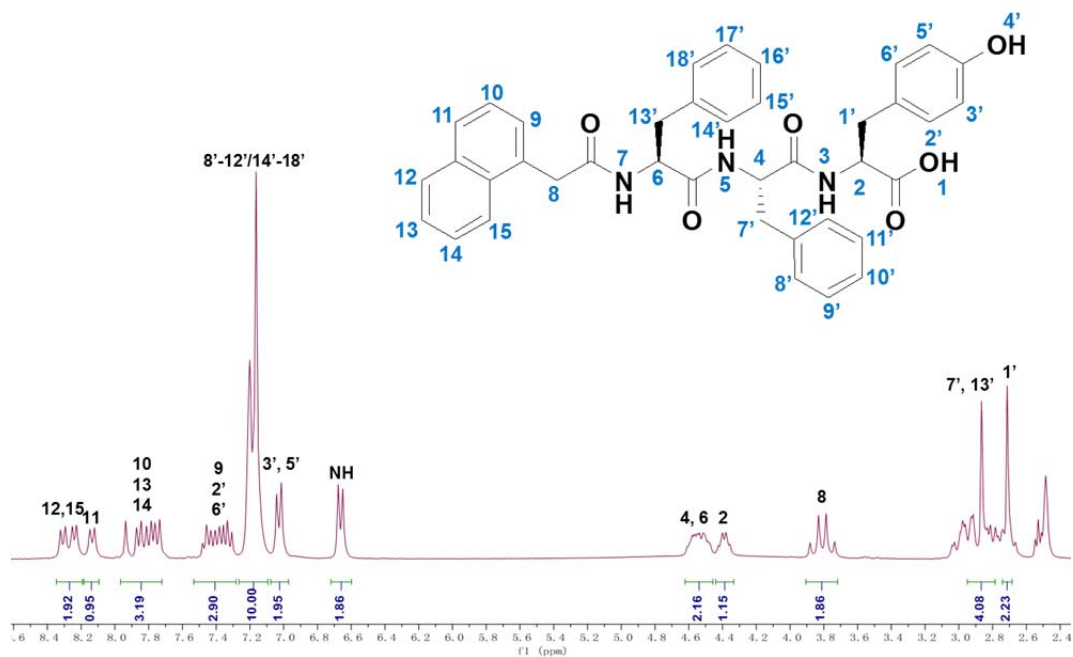


Figure S5. ^1H NMR spectrum of **1**.

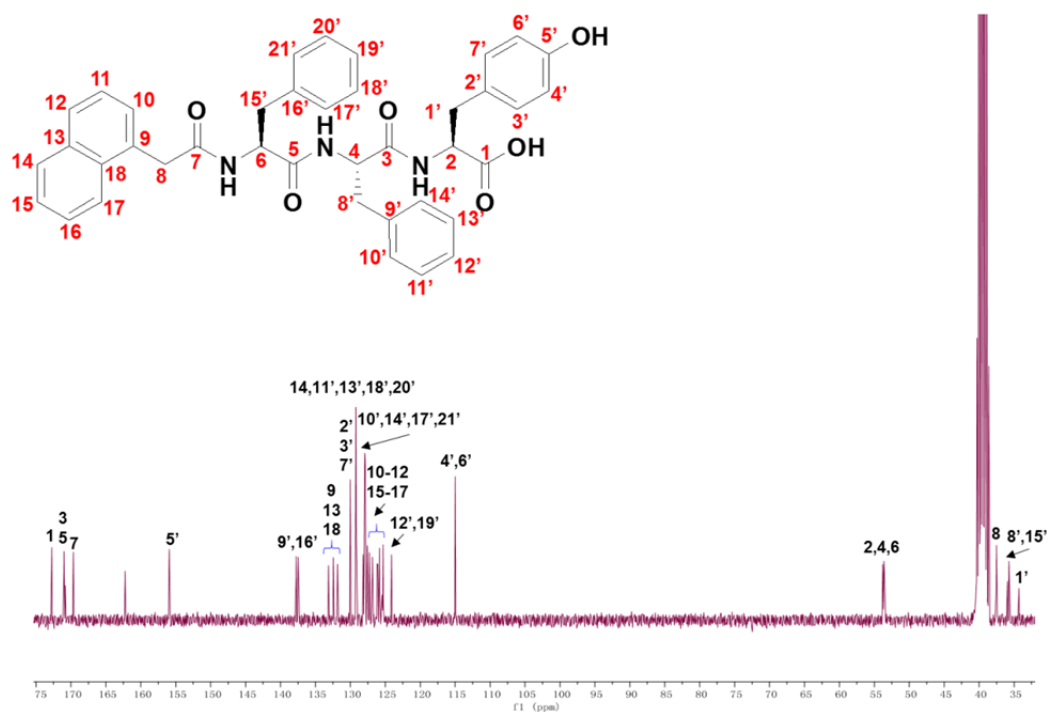


Figure S6. ^{13}C NMR spectrum of **1**.

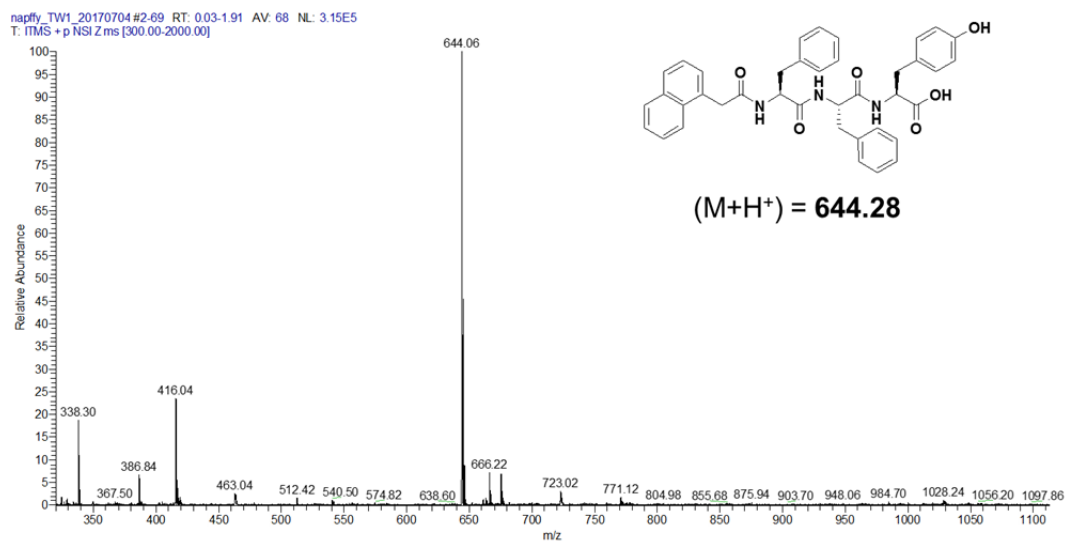


Figure S7. ESI-MS spectrum of **1**.

3. Supporting figures and tables.

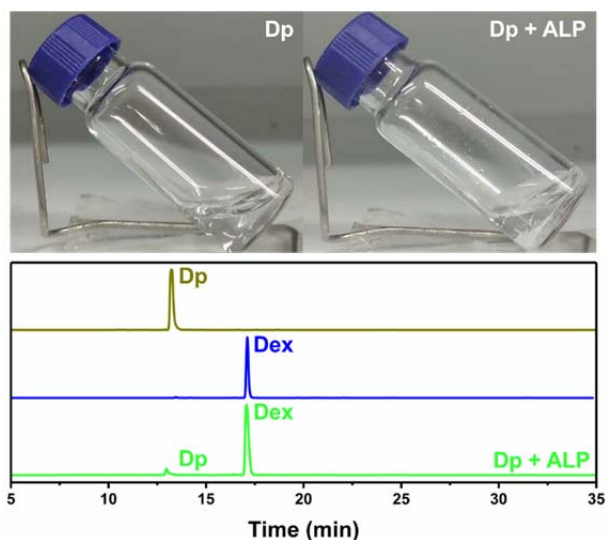


Figure S8. Photographs of solution of **Dp** at 0.7 wt% (left), **Dp** at 0.7 wt% incubated with 0.2 unit/ μ L ALP (right) for 8 h at 37 °C (top). HPLC traces of **Dp** (caramel), **Dex** (blue), and **Dp** with ALP (green). Wavelength for detection: 268 nm.

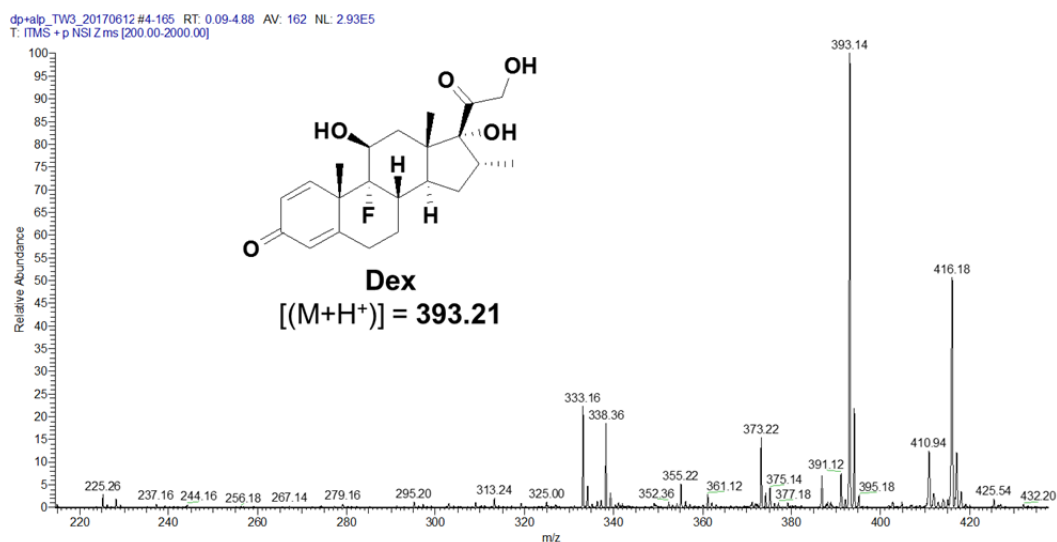


Figure S9. ESI-MS spectrum of the peak at 17.1 min on the **Dp** + ALP HPLC trace in Figure S8.

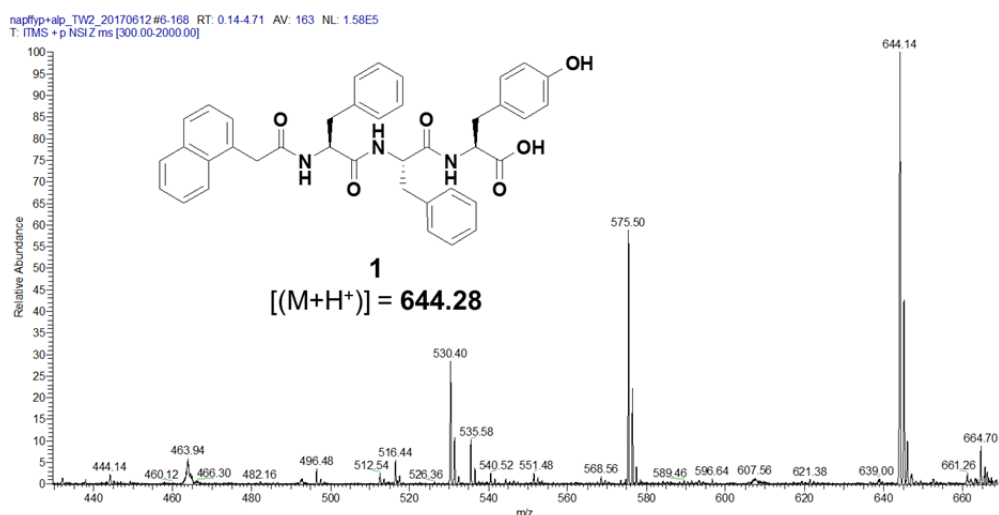


Figure S10. ESI-MS spectrum of the peak at 25.1 min on the HPLC trace of **Gel 1** in Figure 2b.

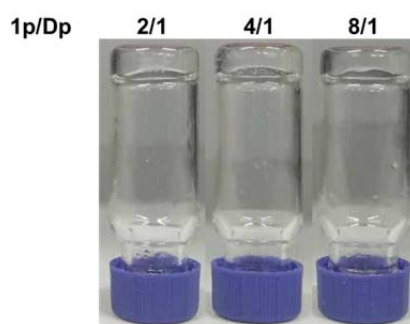


Figure S11. Photographs of Gel 2 hydrogels at fixed **1p** concentration of 1.0 wt% and different **1p** : **Dp** ratios.

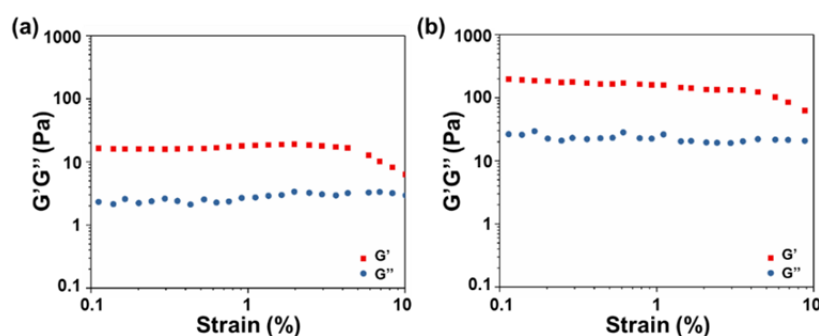


Figure S12. (a) Dynamic strain of storage modulus (G') and the loss modulus (G'') of Gel 1 at the frequency of 1 Hz, Condition: pH 7.4, 25 °C. (b) Dynamic strain of storage modulus (G') and the loss modulus (G'') of Gel 2 at the frequency of 1 Hz, Condition: pH 7.4, 25 °C.

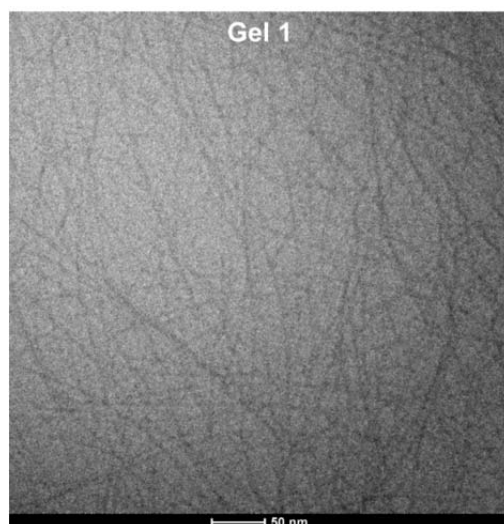


Figure S13. Cryo-TEM image of the nanofibers in Gel 1 formed by treating the 1.0 wt% **1p** solution with 0.2 unit/ μ L ALP in phosphate buffer at 37 °C for 8 h. Scale bar, 50 nm.

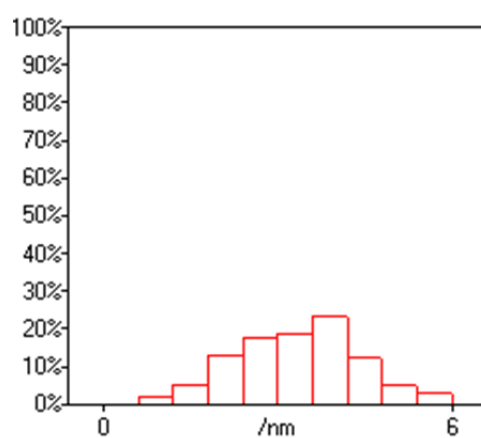


Figure S14. Statistic graph of the nanofiber diameters in Figure 3c.

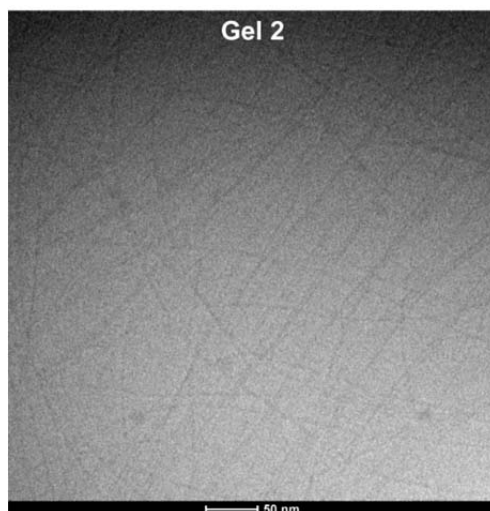


Figure S15. Cryo-TEM image of the nanofibers in Gel **2** formed by treating the 1.0 wt% **1p** and molar equivalent **Dp** solution with 0.2 unit/ μ L ALP in phosphate buffer at 37 °C for 8 h. Scale bar, 50 nm.

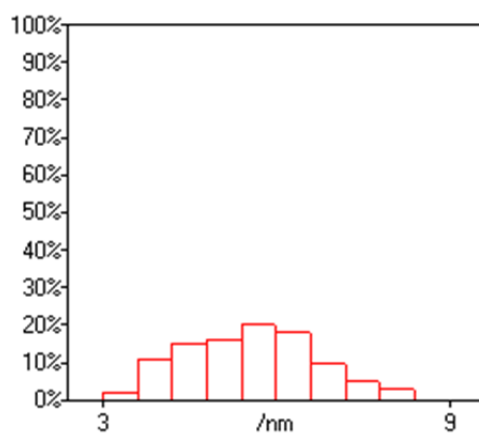


Figure S16. Statistic graph of the nanofiber diameters in Figure 3d.

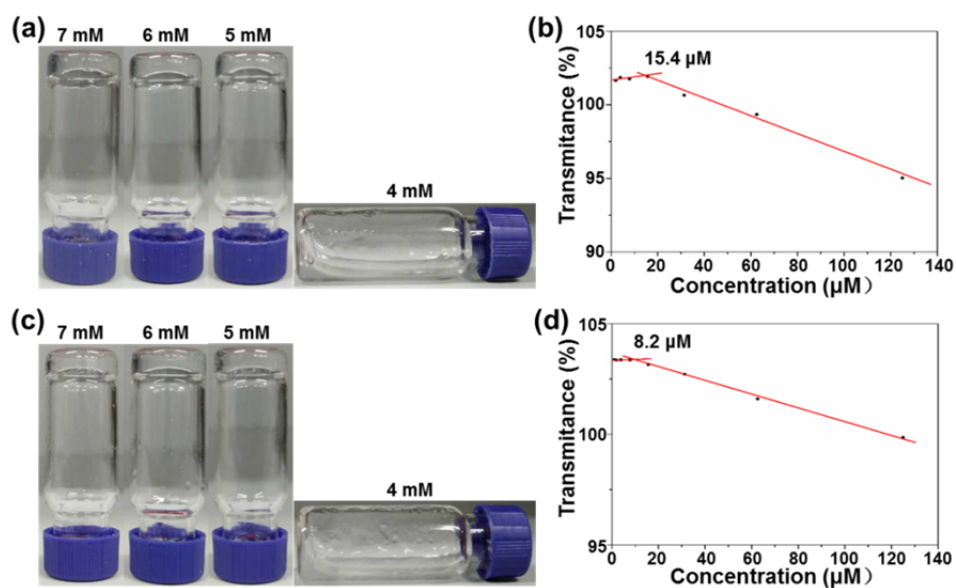


Figure S17. (a) Critical gelation concentration (CGC) determination. Inverted tube test indicated that the CGC for **Gel 1** was 4.5 ± 0.5 mM. (b) Gelator concentration-dependent transmittance at 600 nm of dilutions of **Gel 1**. (c) Inverted tube test indicated that the CGC for **Gel 2** was 4.5 ± 0.5 mM. (d) Gelator concentration-dependent transmittance at 600 nm of dilutions of **Gel 2**.

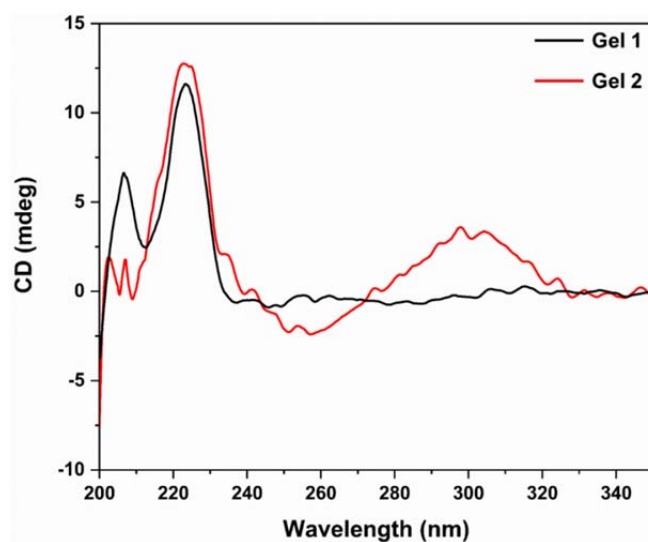


Figure S18. Circular dichroism (CD) spectra of Gel 1 (black) and Gel 2 (red).

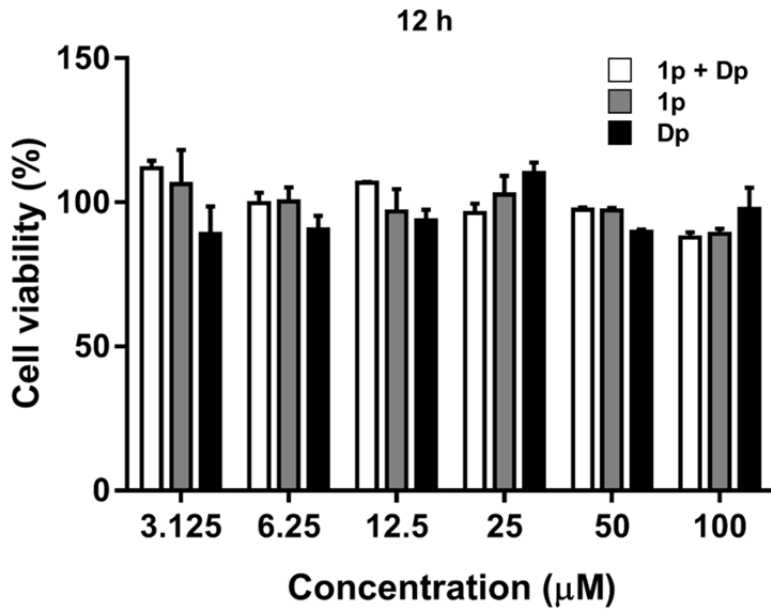


Figure S19. MTT assay of different compounds on LPS-stimulated BMDMs after 12 h incubation.

These experiments were performed in triplicate. Error bars represent standard error of mean (SEM).

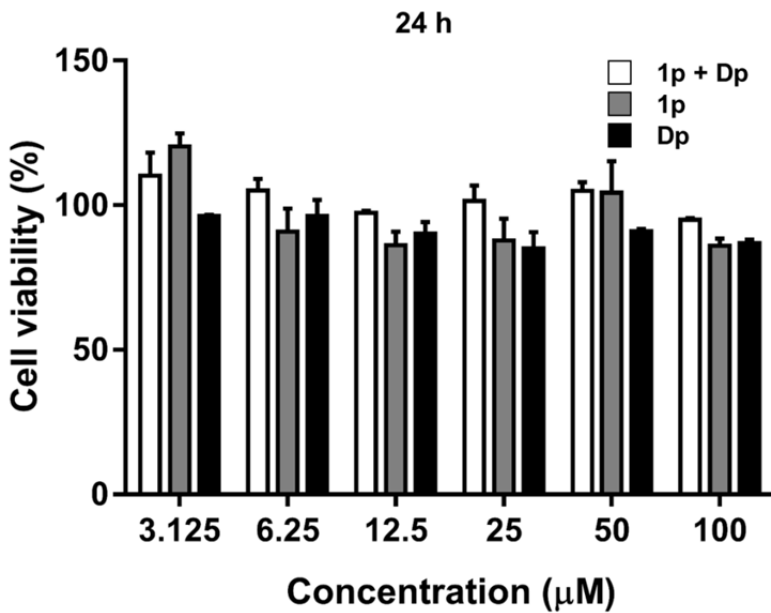


Figure S20. MTT assay of different compounds on LPS-stimulated BMDMs after 24 h incubation.

These experiments were performed in triplicate. Error bars represent SEM.

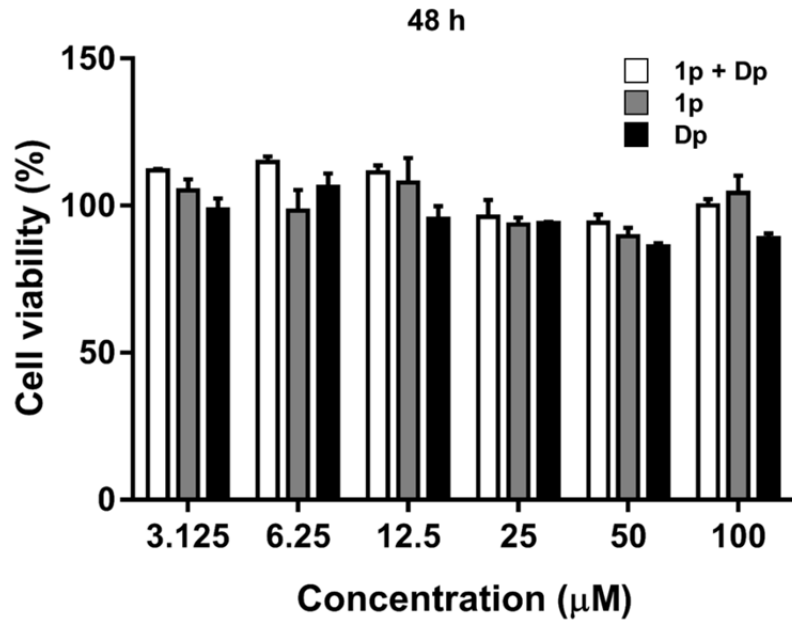


Figure S21. MTT assay of different compounds on LPS-stimulated BMDMs after 48 h incubation.

These experiments were performed in triplicate. Error bars represent SEM.

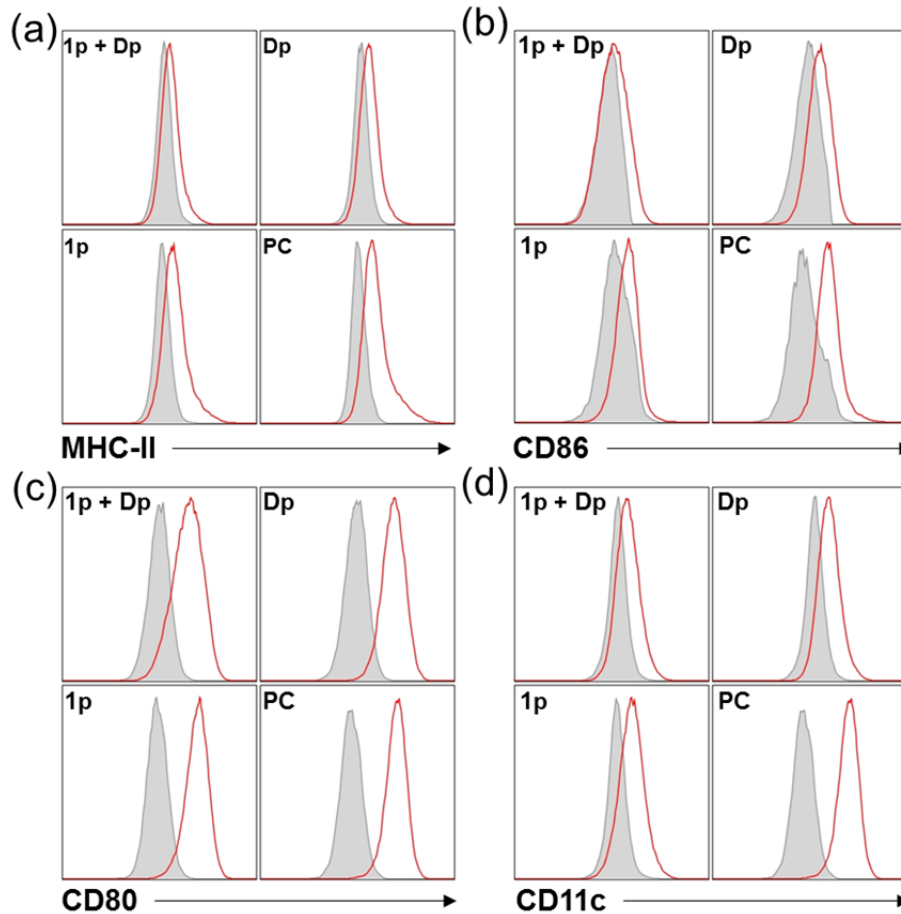


Figure S22. Representative flow cytometric profiles of the expressions of MHC-II (a), CD86 (b), CD80 (c) or CD11c (d) in the F4/80+ CD11b+ gated population of LPS-stimulated BMDMs incubated with different compounds (i.e., **1p** and **Dp**, **Dp**, or **1p**) at 25 μ M for 24 h. PC, positive control.

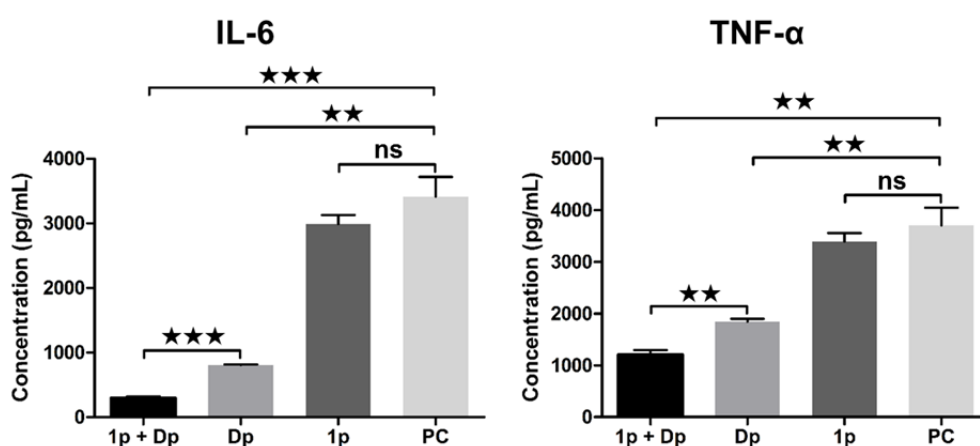


Figure S23. Cytometric Bead Array (CBA) assay of culture medium inflammation cytokine levels in different BMDMs groups. LPS-stimulating BMDMs incubated with different compounds (i.e., **1p** and **Dp**, **Dp**, or **1p**) at 25 μ M for 24 h, then culture medium was collected and inflammation cytokines were measured. PC, positive control. **p < 0.01, ***p < 0.001; ns, not significant.

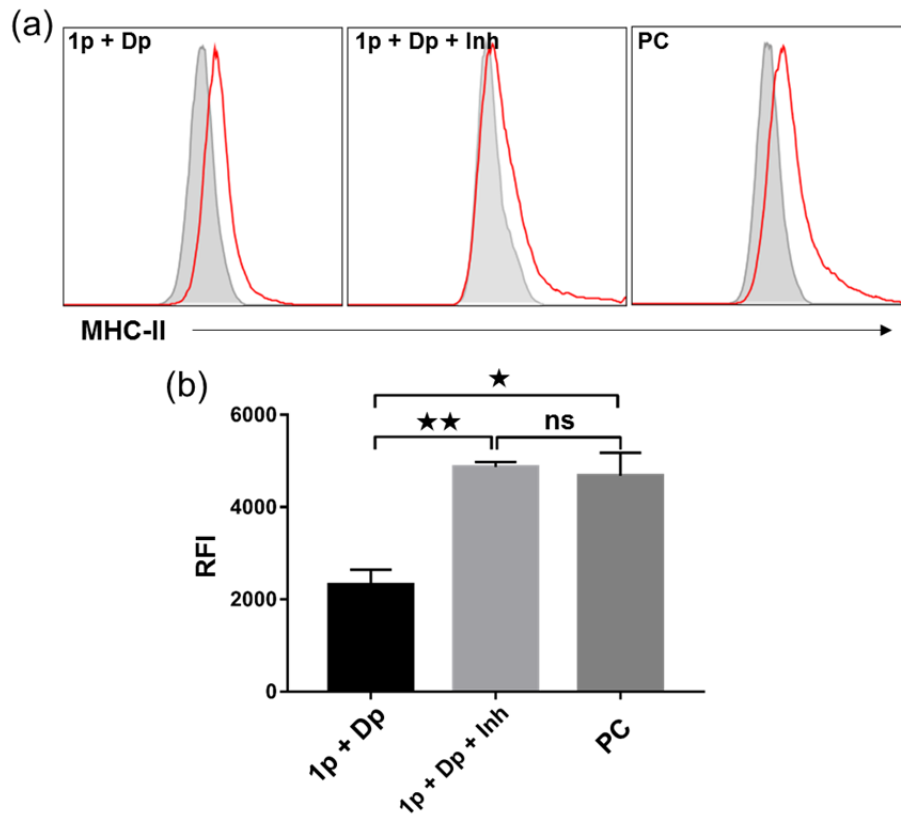


Figure S24. (a) Representative flow cytometric profiles of MHC-II expression in the F4/80+ CD11b+ gated population of LPS-stimulated BMDMs incubated with 25 μ M **1p** and 25 μ M **Dp** for 24 h (left), 25 μ M **1p**, 25 μ M **Dp**, with ALP inhibitor (Inh) for 24 h (middle), and positive control (PC, right). (b) Summary graph of the relative fluorescence intensity (RFI) data in a. The result is illustrated as the mean \pm SEM of the RFI of the F4/80+ CD11b+ MHC-II+-gated LPS-stimulated BMDMs. * $p < 0.05$, ** $p < 0.01$; ns, not significant.

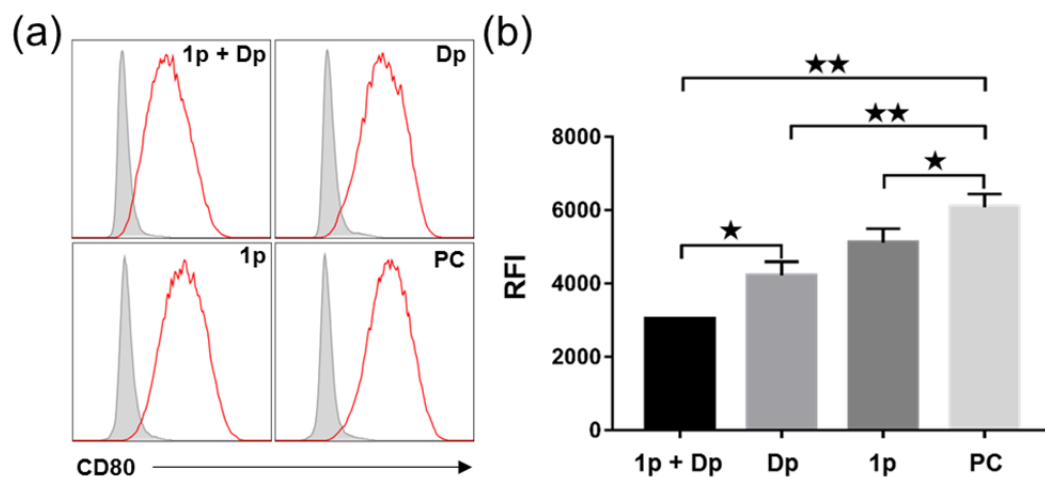


Figure S25. (a) Representative flow cytometric profiles of CD80 expression in the F4/80+ CD11b+-gated population of LPS-stimulated iBMDMs incubated with different compounds (i.e., **1p** and **Dp**, **Dp**, or **Dp**) at 25 μ M for 24 h. (b) Summary graph of the relative fluorescence intensity (RFI) data in a. The results are illustrated as the mean \pm SEM of the RFI of the F4/80+ CD11b+ CD80+ cells. *p < 0.05, **p < 0.01.

Table S1. HPLC condition for the purifications of **1P** and **1**, and Figure 2.

Time (minute)	Flow (mL/min.)	H ₂ O % (0.1%TFA)	CH ₃ CN % (0.1%TFA)
0	3.0	80	20
3	3.0	80	20
35	3.0	20	80
37	3.0	20	80
38	3.0	80	20
40	3.0	80	20

Reference:

- 1 X. Q. Wang, W. Jiang, Y. Q. Yan, T. Gong, J. H. Han, Z. G. Tian and R. B. Zhou, *Nat. Immunol.*, 2014, **15**, 1126-1133.